Contribution from the Department of Chemistry, The University
of Western Ontario, London, Ontario, Canada N6A 5B7

Synthesis, Structure, and Reactivity of Pt_3Au and Pt_3Au_2 Cluster Complexes

Nicholas C. Payne, Ravindranath Ramachandran, Guy Schoettel, Jagadese J. Vittal,
and Richard J. Puddephatt*

Received March 19, 1991

The complex $[Pt_3(\mu_3\text{-}H)(\mu\text{-dppm})_3]^+$ (dppm = $Ph_2PCH_2PPh_2$) reacts with LAu^+ (L = PPh_3) to give $[Pt_3(\mu_3\text{-}H)(\mu_3\text{-AuL})(\mu\text{-dppm})_3]^{2+}$ and with excess LAu^+ to give $[Pt_3(\mu_3\text{-AuL})_2(\mu\text{-dppm})_3]^{2+}$. The complex $[Pt_3(\mu_3\text{-}H)(\mu_3\text{-AuL})(\mu\text{-dppm})_3]^{2+}$ can be reversibly deprotonated to give $[Pt_3(\mu_3\text{-AuL})(\mu\text{-dppm})_3]^+$; this reacts with LAu^+ to give $[Pt_3(\mu_3\text{-AuL})_2(\mu\text{-dppm})_3]^{2+}$, from which one LAu^+ unit can be removed as L_2Au^+ by reaction with free L to regenerate $[Pt_3(\mu_3\text{-AuL})(\mu\text{-dppm})_3]^+$. These reactions indicate clearly how electrophilic substitution at a triplatinum center can occur by a stepwise mechanism (S_E2 stepwise). The complexes $[Pt_3(\mu_3\text{-AuL})(\mu\text{-dppm})_3]^+$ (L = PPh_3) and $[Pt_3(\mu_3\text{-AuL})_2(\mu\text{-dppm})_3]^{2+}$ (L = PMe_3) can be prepared most conveniently by reaction of $[Pt_3(\mu_3\text{-CO})(\mu\text{-dppm})_3]^{2+}$ with LAuCl (or LAuBr) and $NaBH_4$. The silver complex $[Pt_3(\mu_3\text{-}H)(\mu_3\text{-AgPPh}_3)(\mu\text{-dppm})_3][PF_6]_2$ is much less thermally stable than the gold analogue. The complex $[Pt_3(\mu_3\text{-AuPPh}_3)(\mu\text{-dppm})_3]^+$ reversibly adds CO to give $[Pt_3(CO)(\mu_3\text{-AuPPh}_3)(\mu\text{-dppm})_3]^+$; the carbonyl ligand is terminal with $\nu(CO) = 1995\ cm^{-1}$, but it migrates rapidly around the Pt_3 triangle even at −90 °C so that, by NMR spectroscopy, the molecule appears to have 3-fold symmetry. The complexes were characterized by multinuclear NMR methods and $[Pt_3(\mu_3\text{-AuPMe}_3)_2(\mu\text{-dppm})_3][PF_6]_2$ was also characterized crystallographically [space group $P2_1/c$, $Z = 4$, $a = 14.442\ (2)$ Å, $b = 26.676\ (2)$ Å, $c = 25.749\ (2)$ Å, $\beta = 104.117\ (8)°$, $R = 0.049$]. It is the first example of a Pt_3Au_2 cluster with this electron count, and the Pt_3Au_2 core is trigonal bipyramidal with Pt–Pt distances ranging from 2.635 (1) to 2.642 (1) Å and Pt–Au distances ranging much more widely from 2.678 (1) to 2.843 (1) Å.

Introduction

The first well-defined PtAu cluster complexes were prepared in 1984, and since that time, an impressive array of such complexes have been synthesized and characterized.[1-13] Of particular interest with respect to the present work are Pt_3Au and Pt_3Au_2 complexes, such as $[Pt_3(\mu\text{-CO})_3L_3(\mu_3\text{-AuL})]^+$ (**1**),[2] $[Pt_3(\mu\text{-CO})_2(\mu\text{-SO}_2)L_3(\mu_3\text{-AuL})]^+$ (**2**),[3] $[Pt_3(\mu\text{-Cl})(\mu\text{-SO}_2)_2L_3(\mu_3\text{-AuL}^1)]$ (**3**),[3] $[Pt_3(\mu\text{-Cl})(\mu\text{-SO}_2)_2L_3(\mu_3\text{-AuL}^1)_2]^+$ (**4**),[3] [L = PCy_3, $L^1 = P(4\text{-FC}_6H_4)_3$], and $[Pt_3(\mu\text{-CO})_3L_4(\mu_3\text{-AuL})]^+$ (**5**;[12] L = PPh_3), which are formed by addition of AuL^+ fragments to 42-electron or 44-electron Pt_3 clusters. This work reports related derivatives based on the $Pt_3(\mu\text{-dppm})_3$ cluster building block, including the structure of the first Pt_3Au_2 cluster based on a 42-electron Pt_3 unit. It also gives some reactions of the platinum–gold clusters. A preliminary account of part of this work has been published.[14]

Results

Synthesis of New Clusters. The new platinum–gold clusters, containing Ph_3PAu units, were prepared from $[Pt_3(\mu_3\text{-CO})(\mu\text{-dppm})_3]^{2+}$ (**6**)[15] and $[Pt_3(\mu_3\text{-}H)(\mu\text{-dppm})_3]^+$ (**7**),[16] as shown in Scheme I, in which the μ-dppm = μ-$Ph_2PCH_2PPh_2$ ligands have been omitted for clarity. Treatment of complex **7** with LAu^+ (L = PPh_3) gave $[Pt_3(\mu_3\text{-}H)(\mu_3\text{-AuL})(\mu\text{-dppm})_3]^{2+}$ (**8**). Complex **8** was easily deprotonated to give $[Pt_3(\mu_3\text{-AuL})(\mu\text{-dppm})_3]^+$ (**9**), and **9** was easily protonated to give back **8**. The overall conversion of **7** to give **9** involves the isolobal substitution of LAu^+ for H^+, which is now a well-known process,[17] but it is relatively unusual for the intermediate product, in this case **8**, to be isolated from such reactions.[4-6,18] The overall process may be described as an S_E2 (stepwise) substitution mechanism. Complex **9** could be prepared more simply by reaction of **6** and $[AuCl(PPh_3)]$ with $Na[BH_4]$ (Scheme I), and this synthesis is preferred, since it does not require the synthesis of the sensitive complex $[Pt_3(\mu_3\text{-}H)(\mu\text{-dppm})_3]^+$.

Complex **9** reacted easily with more LAu^+ to give $[Pt_3(\mu_3\text{-AuL})_2(\mu\text{-dppm})_3]^{2+}$ (**10a**; L = PPh_3), and this complex was also

Scheme I

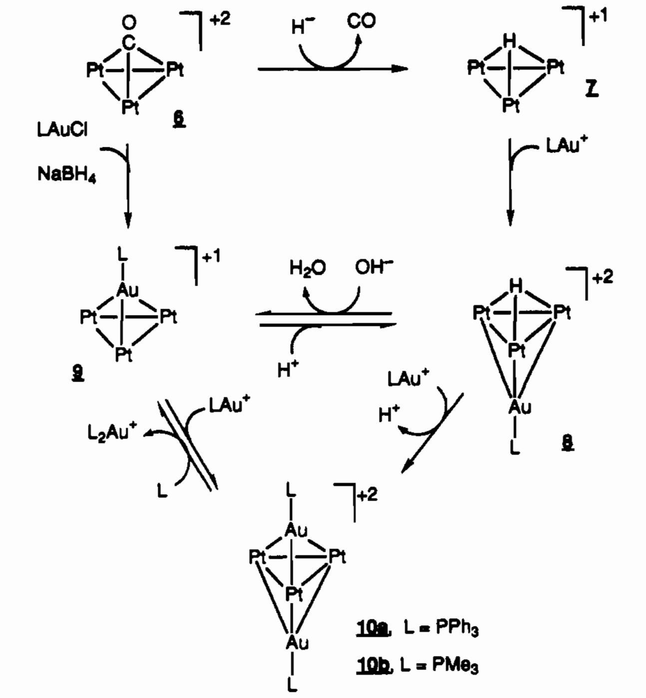

---

(1) Braunstein, P.; Lehner, H.; Matt, D.; Tiripicchio, A.; Tiripicchio-Camellini, M. *Angew Chem., Int. Ed. Engl.* **1984**, *23*, 304.
(2) Briant, C. E.; Wardle, R. W. M.; Mingos, D. M. P. *J. Organomet. Chem.* **1984**, *267*, C49.
(3) (a) Mingos, D. M. P.; Wardle, R. W. M. *J. Chem. Soc., Dalton Trans.* **1986**, 73. (b) Mingos, D. M. P.; Oster, P.; Sherman, D. J. *J. Organomet. Chem.* **1987**, *320*, 257.
(4) Mueting, A. M.; Bos, W.; Alexander, B. D.; Boyle, P. D.; Casalnuovo, J. A.; Balaban, S.; Ho, L. N.; Johnson, S. M.; Pignolet, L. H. *New J. Chem.* **1988**, *12*, 505.
(5) Braunstein, P.; Rose, J. *Gold Bull.* **1985**, *18*, 17.
(6) Hall, K. P.; Mingos, D. M. P. *Prog. Inorg. Chem.* **1984**, *32*, 237.
(7) Bour, J. J.; Berg, W. v. d.; Schlebos, P. P. J.; Kanters, R. P. F.; Schoondergang, M. F. J.; Bosman, W. P.; Smits, J. M. M.; Beurskens, P. T.; Steggerda, J. J.; van der Sluis, P. *Inorg. Chem.* **1990**, *29*, 2971.
(8) Ho, L. N.; Sweet, J. D.; Mueting, A. M.; Pignolet, L. H.; Schoondergang, M. F. J.; Steggerda, J. J. *Inorg. Chem.* **1989**, *28*, 3696.
(9) Bennett, M. A.; Berry, D. E.; Beveridge, K. A. *Inorg. Chem.* **1990**, *29*, 4148.
(10) Hallam, M. F.; Mingos, D. M. P.; Adatia, T.; McPartlin, M. *J. Chem. Soc., Dalton Trans.* **1988**, 335.
(11) Bender, R.; Braunstein, P.; Dedieu, A.; Dusausoy, Y. *Angew. Chem., Int. Ed. Engl.* **1989**, *28*, 923.
(12) Bour, J. J.; Kanters, R. P. E.; Schlebos, P. P. J.; Bos, W.; Bosman, W. P.; Behm, H.; Beurskens, P. T.; Steggerda, J. J. *J. Organomet. Chem.* **1987**, *329*, 405.
(13) (a) Smith, D. E.; Welch, A. J.; Treurnicht, I.; Puddephatt, R. J. *Inorg. Chem.* **1986**, *25*, 4617. (b) Manojlovic-Muir, Lj.; Muir, K. W.; Treurnicht, I.; Puddephatt, R. J. *Inorg. Chem.* **1987**, *26*, 2418. (c) Arsenault, G. J.; Puddephatt, R. J. *Can. J. Chem.* **1989**, *67*, 1800.
(14) Ramachandran, R.; Payne, N. C.; Puddephatt, R. J. *J. Chem. Soc., Chem. Commun.* **1989**, 128.
(15) Ferguson, G.; Lloyd, B. R.; Puddephatt, R. J. *Organometallics* **1986**, *5*, 344.
(16) Lloyd, B. R.; Puddephatt, R. J. *J. Am. Chem. Soc.* **1985**, *107*, 7785.
(17) Lauher, J.; Wald, K. *J. Am. Chem. Soc.* **1981**, *103*, 7648.
(18) Puddephatt, R. J. In *Comprehensive Coordination Chemistry*; Wilkinson, G., Ed.; Pergamon: Oxford, U.K., 1987; Vol. 5, Chapter 55.

0020-1669/91/1330-4048$02.50/0

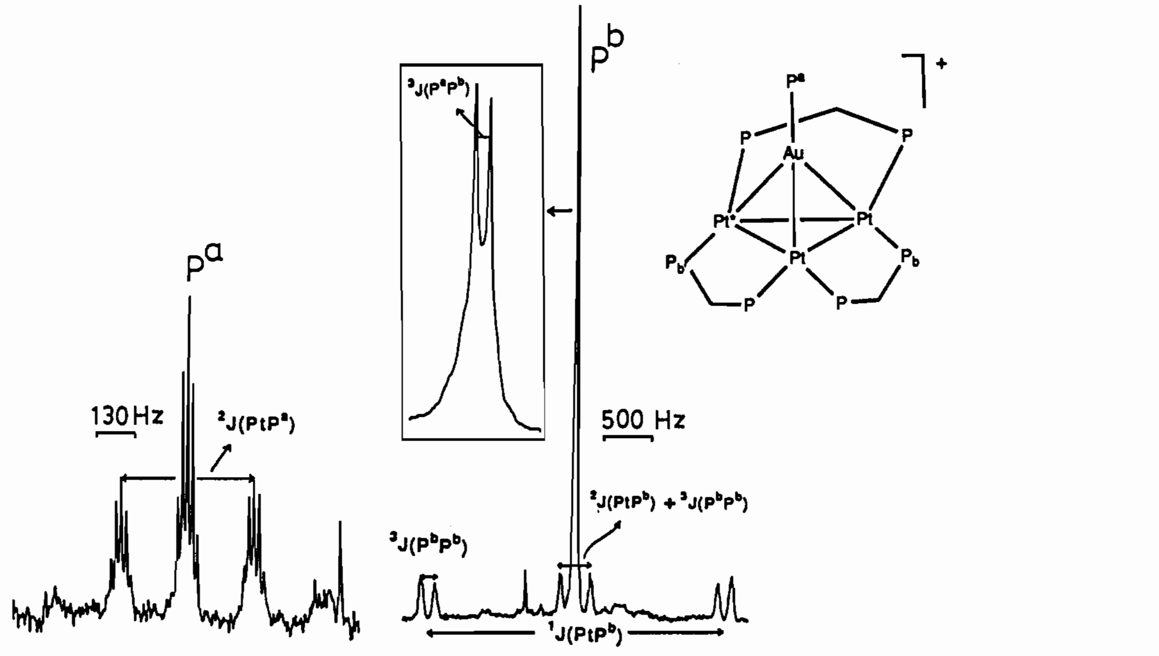

Figure 1. ^{31}P NMR spectrum (121.4 MHz) of complex **8**. The P^a resonance is expected to be a 1:12:49:84:49:12:1 septet due to ^{195}Pt coupling, but as usual for triply bridging groups, only the inner five lines are observed as an apparent 1:4:7:4:1 quintet. The small septet coupling in the P^a resonance is due to $^3J(P^aP^b)$, and this coupling is also observed in the P^b resonance (an expansion is shown in the inset).

prepared by substitution of LAu^+ for H^+ in complex **8**. One LAu^+ fragment could be removed from **10a** as $[AuL_2]^+$ by reaction with L = triphenylphosphine, but the second gold atom could not be removed in this way. A similar complex, $[Pt_3(\mu_3\text{-}AuL)_2(\mu\text{-}dppm)_3]^{2+}$ (L = PMe_3; **10b**), could be prepared in a single step by reaction of **6** and $[AuCl(PMe_3)]$ with $NaBH_4$. Complex **10a** could not be prepared in the analogous way; even with excess $[AuCl(PPh_3)]$, the only product was **9** and the excess $[AuCl(PPh_3)]$ was reduced to metallic gold. The removal of gold fragments from gold-containing clusters by reaction with nucleophiles is a well-known process, and the above chemistry adds to this body of knowledge.[4]

The Pt_3Au clusters have good thermal stability, but attempts to synthesize similar copper and silver derivatives have been less successful. A silver complex **11** (L = PPh_3) could be synthesized (eq 1, L = PPh_3) and characterized by its NMR spectra, but it had low thermal stability and good analytical data could not be obtained. For this reason, its chemistry has not been studied in detail.

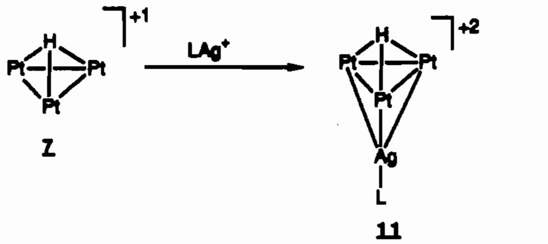

(1)

A silver-bridged cluster complex $[Ag\{Pt_3(\mu\text{-}CO)_3L_3\}_2]^+$ (L = P-*i*-Pr_3) has been characterized previously,[19] as has the complex $[Pt_3(\mu\text{-}CO)_3L_4(\mu_3\text{-}AgL)]^+$ (L = PPh_3).[20]

Characterization of the Complexes. The complexes were characterized by their FAB mass spectra, which usually contained a parent ion peak, and by multinuclear NMR methods. Complex **10b** was characterized crystallographically.

Table I. ^1H, ^{31}P, and ^{195}Pt NMR Data for the Clusters[a]

	7	8	9	10a	10b	11	12[e]
δ(Pa)		44.6	46.3	44.4	−4.96	16.5[b]	41.8
$^2J(PtP^a)$		503	892	440	451	335	620
$^3J(P^aP^b)$		19	22.5	21	0	8.5	0
$\delta(P^b)$		−13.4	−12.6	−16.0	−5.1	−14.5	−14.3
$^1J(PtP^b)$		3155	3020	3060	2827	3139	2922
$^2J(PtP^b)$		170	190	134	254	182	212
$^3J(P^bP^{b1})$		150	200	170	236	155	204
$\delta(^{195}Pt)$		−2463	*c*	−2207	−2542	−2504	*c*
δ(PtH)	4.16	−0.90[d]				−1.11	
$^1J(PtH)$	710	317				325	
$^2J(P^bH)$	23	17				16	
$\delta(CH_2P_2)$	5.02 5.61	5.00 6.40	4.11 6.50	5.20	5.54	5.14 6.20	4.71 5.83[f]
$^2J(H^aH^b)$	14	14	10			11	14

[a] See Figure 1 for notation. [b] $^1J(^{107}AgP^a)$ = 536 Hz, $^1J(^{109}AgP^a)$ = 550 Hz, $^2J(AgP^b)$ = 21 Hz. [c] Not recorded. [d] $^3J(P^aH)$ = 11.5 Hz. [e] $\delta(^{13}CO)$ = 204.0 ppm, $^1J(PtC)$ = 368 Hz, $^3J(P^aC)$ = 48 Hz. [f] $J(PtH)$ = 78 Hz.

The NMR data are given in Table I, and typical spectra are given in Figure 1 and in Figures S1 and S2 (supplementary material). In the ^1H NMR spectra, the CH_2 protons of the dppm ligands appeared as "AB" multiplets for complexes **8**, **9**, and **11**, which have no plane of symmetry containing the $Pt_3P_6C_3$ atoms, but as a single resonance for **10a** and **10b**, which do have such a symmetry plane. Complexes **8** and **11** also gave resonances due to the $Pt_3(\mu_3\text{-}H)$ group, which appeared as apparent 1:4:7:4:1 quintets due to coupling to ^{195}Pt, as expected for the inner five lines of the calculated 1:12:49:84:49:12:1 septet (the outer lines are too weak to observe) for a $Pt_3(\mu_3\text{-}H)$ group. It is significant that the coupling constants $^1J(PtH)$ for **8** (317 Hz) and **11** (325 Hz) are only about half the value for the parent **7** (710 Hz).[16]

The ^{31}P NMR spectra were particularly useful for structure determination. Thus the spectrum of **9** (Figure 1) contained two resonances, a doublet for the dppm phosphorus atoms and a septet for the Ph_3PAu phosphorus atom due to PP coupling. This immediately proves that 3-fold symmetry is maintained and that there is just one Ph_3PAu unit present. The Ph_3PAu resonance appeared as a 1:4:7:4:1 quintet due to the coupling $^2J(PtAuP)$, confirming that the Ph_3PAu unit is triply bridging. The ^{31}P NMR spectra

---

(19) Albinati, A.; Dahmen, K.-H.; Togni, A.; Venanzi, L. M. *Angew. Chem., Int. Ed. Engl.* **1985**, *24*, 766.
(20) Bhaduri, S.; Sharma, K.; Jones, P. G.; Erdbrügger, C. E. *J. Organomet. Chem.* **1987**, *326*, C46.

Table II. Selected Bond Distances (Å) and Angles (deg)

Au(1)-Pt(1)	2.761 (1)	Au(1)-Pt(2)	2.767 (1)
Au(1)-Pt(3)	2.714 (1)	Au(2)-Pt(1)	2.707 (1)
Au(2)-Pt(2)	2.678 (1)	Au(2)-Pt(3)	2.843 (1)
Pt(1)-Pt(2)	2.640 (1)	Pt(1)-Pt(3)	2.635 (1)
Pt(2)-Pt(3)	2.642 (1)	Au(1)-P(1)	2.221 (4)
Au(2)-P(2)	2.248 (4)	Pt(1)-P(3)	2.292 (4)
Pt(2)-P(4)	2.286 (4)	Pt(2)-P(5)	2.284 (4)
Pt(3)-P(6)	2.287 (4)	Pt(3)-P(7)	2.301 (4)
Pt(1)-P(8)	2.268 (4)		
Pt(2)-Au(1)-Pt(1)	57.06 (2)	Pt(3)-Au(1)-Pt(1)	57.53 (2)
Pt(3)-Au(1)-Pt(2)	57.62 (2)	P(1)-Au(1)-Pt(1)	147.2 (1)
P(1)-Au(1)-Pt(2)	140.9 (1)	P(1)-Au(1)-Pt(3)	150.2 (1)
Pt(2)-Au(2)-Pt(1)	58.72 (2)	Pt(3)-Au(2)-Pt(1)	56.62 (2)
Pt(3)-Au(2)-Pt(2)	57.08 (2)	P(2)-Au(2)-Pt(1)	146.7 (1)
P(2)-Au(2)-Pt(2)	147.7 (1)	P(2)-Au(2)-Pt(3)	144.2 (1)
Au(1)-Pt(1)-Pt(2)	61.59 (2)	Au(1)-Pt(1)-Pt(3)	60.33 (2)
Au(2)-Pt(1)-Pt(2)	60.09 (2)	Au(2)-Pt(1)-Pt(3)	64.30 (2)
Au(2)-Pt(1)-Au(1)	113.25 (3)	Pt(3)-Pt(1)-Pt(2)	60.10 (2)
P(3)-Pt(1)-Pt(2)	96.5 (1)	P(3)-Pt(1)-Pt(3)	156.2 (1)
P(3)-Pt(1)-Au(1)	114.6 (1)	P(3)-Pt(1)-Au(2)	101.5 (1)
P(8)-Pt(1)-Pt(2)	153.1 (1)	P(8)-Pt(1)-Pt(3)	96.0 (1)
P(8)-Pt(1)-Au(1)	97.0 (1)	P(8)-Pt(1)-Au(2)	123.3 (1)
P(8)-Pt(1)-P(3)	107.8 (1)	Pt(3)-Pt(2)-Pt(1)	59.84 (2)
Au(1)-Pt(2)-Pt(1)	61.35 (2)	Au(1)-Pt(2)-Pt(3)	60.17 (2)
Au(2)-Pt(2)-Pt(1)	61.19 (2)	Au(2)-Pt(2)-Pt(3)	64.61 (2)
Au(2)-Pt(2)-Au(1)	113.97 (3)	P(4)-Pt(2)-Pt(1)	93.9 (1)
P(4)-Pt(2)-Pt(3)	153.6 (1)	P(4)-Pt(2)-Au(1)	107.6 (1)
P(4)-Pt(2)-Au(2)	105.9 (1)	P(5)-Pt(2)-Pt(1)	154.8 (1)
P(5)-Pt(2)-Pt(3)	96.0 (1)	P(5)-Pt(2)-Au(1)	101.7 (1)
P(5)-Pt(2)-Au(2)	117.5 (1)	P(5)-Pt(2)-P(4)	109.8 (1)
Pt(2)-Pt(3)-Pt(1)	60.05 (2)	Au(1)-Pt(3)-Pt(1)	62.14 (2)
Au(1)-Pt(3)-Pt(2)	62.21 (2)	Au(2)-Pt(3)-Pt(1)	59.08 (2)
Au(2)-Pt(3)-Pt(2)	58.32 (2)	Au(2)-Pt(3)-Au(1)	110.50 (3)
P(6)-Pt(3)-Pt(1)	153.7 (1)	P(6)-Pt(3)-Pt(2)	94.5 (1)
P(6)-Pt(3)-Au(1)	101.8 (1)	P(6)-Pt(3)-Au(2)	115.0 (1)
P(7)-Pt(3)-Pt(1)	93.5 (1)	P(7)-Pt(3)-Pt(2)	153.2 (1)
P(7)-Pt(3)-Au(1)	103.2 (1)	P(7)-Pt(3)-Au(2)	113.9 (1)
P(7)-Pt(3)-P(6)	111.1 (1)		

of **10a** and **10b** were similar (Figure S1) except that the resonance due to the phosphorus atoms of dppm appeared as a triplet due to coupling to two Ph_3PAu phosphorus atoms. The ^{31}P NMR spectrum of **11** was similar to that of **8** except that extra couplings due to J(AgP) were present and the extra doublet splittings further prove the presence of a single Ph_3PAg unit (Figure S2). The coupling constant ^2J(PtAuP) is much larger for the monocapped cluster **9** (892 Hz) than for the biscapped clusters **8** (503 Hz), **10a** (440 Hz), and **10b** (451 Hz).

The structure of [**10b**]$[PF_6]_2$·2(toluene) was determined by X-ray crystallography, and a view of the cation is shown in Figure 2. Selected bond distances and angles are given in Table II. The Pt_3Au_2 core of the cluster is trigonal bipyramidal with Pt-Pt distances ranging from 2.635 (1) to 2.642 (1) Å and Pt-Au distances ranging from 2.678 (1) to 2.843 (1) Å. The Pt-Au distances cover a much wider range than is normal in symmetrical Pt_3Au clusters (Table III), and this requires some comment. The cavities above and below a $Pt_3(\mu\text{-dppm})_3$ unit, as defined by the ring of phenyl substituents, are usually not equal in size or symmetrical about the center of the Pt_3 triangle. This arises because the μ-dppm ligands adopt an envelope conformation such that phenyl groups on the "flap-up" side are equatorial, whereas on the other side of the Pt_3 triangle they are axial. Complex **10b** (Figure 2) has two dppm ligands with flap-up and one with flap-down conformations, and hence the cavity above will be larger than that below the Pt_3 triangle, although the difference is minimized by displacement of five of the dppm phosphorus atoms above the Pt_3 plane. The shapes of the cavities are such that Pt(3) is least crowded above the plane but most crowded below the plane, and hence Pt(3)-Au(1) is the shortest Pt-Au(1) bond and Pt(3)-Au(2) is the longest Pt-Au(2) bond. Steric effects can

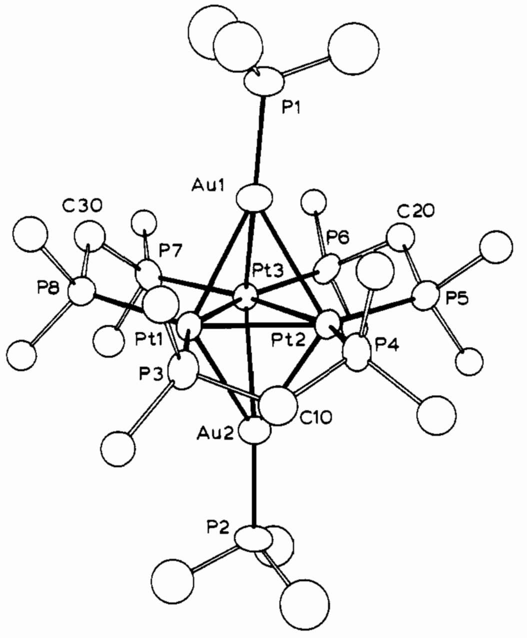

Figure 2. ORTEP view of the structure of the $[Pt_3(\mu\text{-dppm})_3(\mu_3\text{-AuPMe}_3)_2]^{2+}$ cation, showing 50% probability ellipsoids.

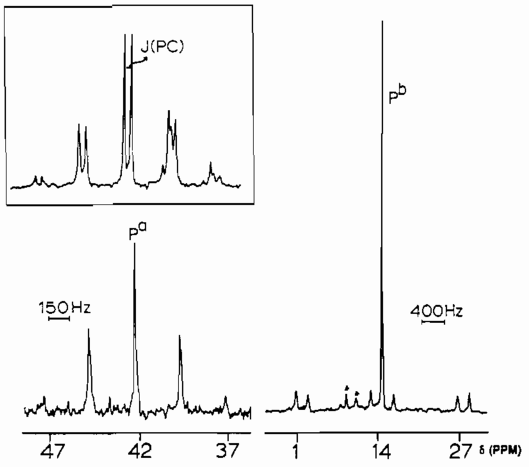

Figure 3. ^{31}P NMR spectrum (121.4 MHz) of complex **12**. The apparent 1:4:7:4:1 quintet appearance of the P^a resonance due to ^1J(PtP) coupling indicates effective 3-fold symmetry of the cluster on the NMR time scale. The inset shows the P^a resonance of the ^{13}CO complex **12***, and the extra doublet splitting is due to ^2J(PC).

Table III. Comparison of Pt-Pt and Pt-Au Bond Distances (Å) in Pt_3Au and Pt_3Au_2 Clusters[2,3,10,12]

complex	e count[a]	Pt-Pt range	mean[b]	Pt-Au range	mean[b]
10b	42 (66)	2.635 (1)-2.642 (1)	2.639	2.678 (1)-2.843 (1)	2.742
1	42 (54)	2.678 (5)-2.705 (6)	2.696	2.750 (5)-2.768 (5)	2.758
2	42 (54)	2.667 (4)-2.746 (1)	2.698	2.755 (1)-2.759 (5)	2.757
3	44 (56)	2.851 (1)-2.872 (1)	2.864	2.766 (1)-2.771 (1)	2.769
4	44 (68)	2.884 (2)-2.888 (2)	2.886	2.772 (2)-2.803 (2)	2.785
5	44 (56)	2.666 (1)-2.708 (1)	2.692	2.700 (1)-2.910 (1)	2.837
14[c]	42 (94)	2.683 (1)-2.683 (1)	2.683	2.725 (1)-2.731 (1)	2.728

[a] The electron count is given for the Pt_3 cluster only, i.e. after removal of the LAu^+ fragments, and, in parentheses, for the Pt_3Au, Pt_3Au_2, or $(Pt_3)_2Au$ cluster cores. [b] The mean has its usual definition; in some cases it should be recognized that individual values are statistically nonequivalent. [c] This complex is $[Au\{Pt_3(\mu\text{-CO})_3L_3\}_2]^+$ (L = PPh_3).[10]

therefore rationalize the trends in Pt–Au distances. The Pt–Pt distances in **10b** are very similar to those for several other $[Pt_3(\mu\text{-dppm})_3]$ complexes,[21-23] and there is no evidence that the gold atoms strengthen or weaken the Pt–Pt bonds. However, both the Pt–Pt and Pt–Au distances in **10b** are shorter than in most other Pt_3Au and Pt_3Au_2 clusters, and this is largely due to the differences in the supporting ligands (Table III). In particular, the presence of μ-CO or μ-SO_2 groups leads to lengthening of Pt–Pt bonds when compared with those of **10b**.

The Carbonyl Complex $[Pt_3(\mu_3\text{-AuPPh}_3)(CO)(\mu\text{-dppm})_3]^+$ (12). Complex **9** reacted reversibly with CO to give the carbonyl complex **12**. This complex was stable only under a CO atmosphere and so was characterized spectroscopically.

The IR spectrum of **12** gave $\nu(CO)$ = 1995 cm^{-1}, and in the ^{13}CO-labeled compound **12***, this band shifted to 1978 cm^{-1}. This frequency indicates that a terminal carbonyl ligand is present. In similar complexes with μ_3-CO ligands, the stretching frequencies are considerably lower. For example, in $[Pt_3(\mu_3\text{-CO})(\mu_3\text{-Hg})(\mu\text{-dppm})_3]^{2+}$, $\nu(CO)$ = 1792 cm^{-1} and, in $[Pt_3(\mu_3\text{-CO})(\mu_3\text{-SnF}_3)(\mu\text{-dppm})_3]^{2+}$, $\nu(CO)$ = 1827 cm^{-1}.[22,23]

The ^{31}P NMR spectrum of **12** is shown in Figure 3. It indicates apparent 3-fold symmetry, since a single resonance was observed for the dppm phosphorus atoms. The inset to Figure 2 shows the Ph_3PAu resonance of **12*** and shows the extra doublet splitting due to the coupling $^3J(PC)$. The ^{13}C NMR spectrum in the carbonyl region is shown in Figure S3 (supplementary material). It appears as a 1:4:7:4:1 quintet of 1:1 doublets due to coupling to ^{195}Pt [$^1J(PtC)$] and ^{31}P [$^2J(P^aC)$], respectively, thus suggesting the presence of a $Pt_3(\mu_3\text{-CO})$ group. No change in the spectra occurred on cooling solutions to −90 °C.

The apparently inconsistent conclusions regarding the structure of **12** based on the IR and NMR data can be rationalized if the complex is fluxional even at −90 °C. Thus the rapid equilibrium in eq 2 is suggested to account for the apparent 3-fold symmetry of the complex suggested by NMR spectroscopy. The transition state would probably have a symmetrical structure **13**, but in the ground state the CO must be terminal (or at best semibridging) and, by comparison with complex **5**,[12] the μ_3-AuL group is likely to be asymmetrically bonded.

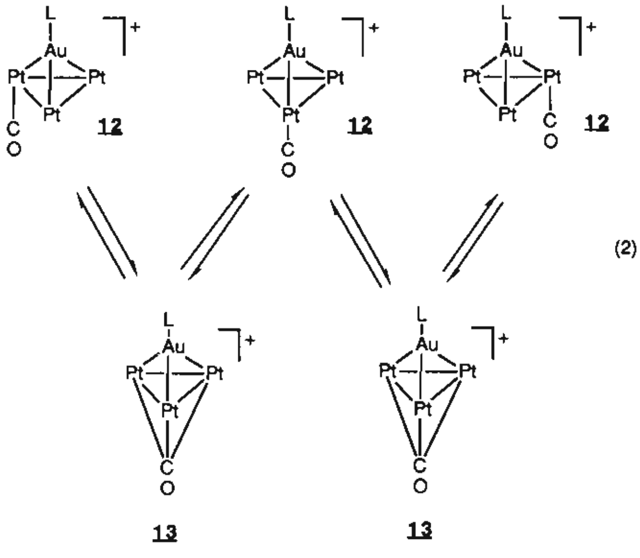

(2)

Discussion

This work has shown that Pt_3Au complexes based on the $Pt_3(\mu\text{-dppm})_3$ unit are stable. In terms of bonding, they may be considered to be formed by donation of electron density from the HOMO of the hypothetical $[Pt_3(\mu\text{-dppm})_3]$ of a_1' symmetry to the vacant a_1' sp-hybrid orbital of a LAu^+ fragment or to the a_1' combination of two such fragments as shown schematically in Figure 4.[6] It follows that the platinum s character involved in a given Pt–Au bond should be approximately half as great in the biscapped clusters **8** and **10** compared to the monocapped clusters **7** and **9**. This accounts nicely for the much reduced values of $^2J(PtP^a)$ in **8** (503 Hz) and **10a** (440 Hz) compared to **9** (892 Hz) and of $^1J(PtH)$ in **8** (317 Hz) compared to **7** (710 Hz).

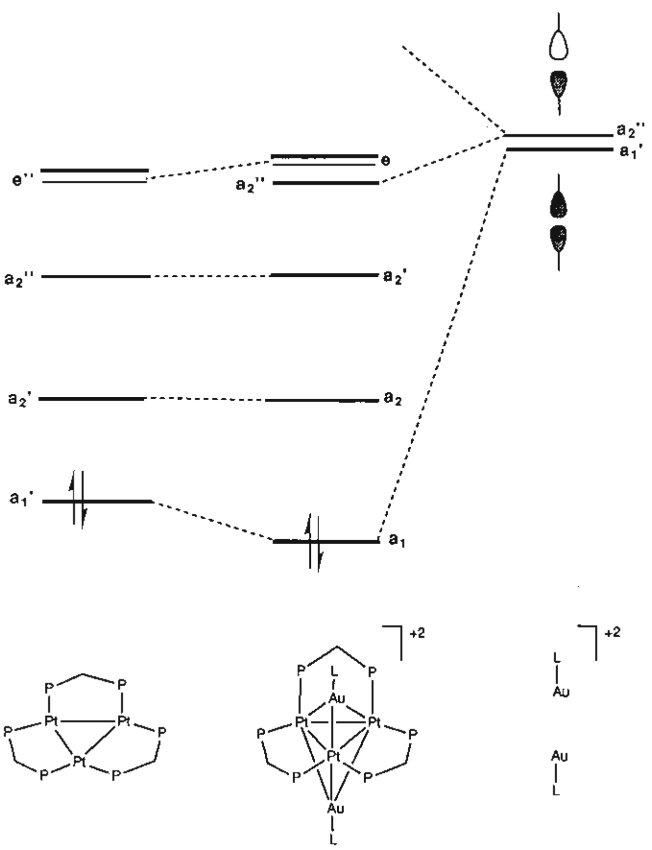

Figure 4. Qualitative MO correlation diagram for the interaction of two LAu^+ fragments with a $Pt_3(\mu\text{-dppm})_3$ fragment, showing the proposed stabilization of the a_1 HOMO.

Cluster **9** has the interesting property of acting as a nucleophile toward H^+ and LAu^+ (Scheme I) in forming **8** and **10** but as an electrophile toward CO (eq 2) in forming **12**. If we consider LAu^+ as a 0-electron ligand, the complexes reported here are 42-electron Pt_3 clusters except for **12**, which is a 44-electron cluster. The only other Pt_3Au_2 cluster to have been characterized is a 44-electron cluster, **4**,[3] and hence **10a,b** are the first 42-electron Pt_3Au_2 clusters.

Experimental Section

NMR spectra were recorded by using a Varian XL200 (^1H) or XL300 (^{13}C, ^{31}P, ^{195}Pt) spectrometer. Chemical shifts are quoted with respect to the standards Me_4Si (^1H, ^{13}C), H_3PO_4 (^{31}P), and K_2PtCl_4 (^{195}Pt). All syntheses were carried out under a dry N_2 atmosphere by using standard Schlenk techniques. The complexes $[Pt_3(\mu_3\text{-H})(\mu\text{-dppm})_3][PF_6]$ and $[Pt_3(\mu_3\text{-CO})(\mu\text{-dppm})_3][PF_6]_2$ were prepared by literature methods.[15,16] Solutions of $[Ph_3PAu(thf)][PF_6]$ in thf were prepared immediately before use by reaction of equimolar amounts of $[AuCl(PPh_3)]$ and $AgPF_6$ in thf for 10 min, followed by filtration to remove precipitated AgCl, while solutions of $[Ph_3PAg(thf)][PF_6]$ were prepared from equimolar amounts of $AgPF_6$ and Ph_3P in thf.

$[Pt_3(\mu_3\text{-H})(\mu_3\text{-AuPPh}_3)(\mu\text{-dppm})_3][PF_6]_2$ (8). To a solution of **7** (46 mg, 0.0246 mmol) in CH_2Cl_2 (5 mL) was added a solution of $[PPh_3Au(thf)][PF_6]$ (15 mg, 0.0248 mmol) in thf (5 mL). The contents were stirred for 1 h. Upon reduction of the volume of solvent and addition of ether (15 mL), a red microcrystalline solid was obtained in 70% yield. Anal. Calcd for $C_{93}H_{82}AuF_{12}P_9Pt_3$: C, 44.9; H, 3.3. Found: C, 44.4; H, 3.4. MP: 190 °C.

$[Pt_3(\mu_3\text{-H})(\mu_3\text{-AgPPh}_3)(\mu\text{-dppm})_3][PF_6]_2$ (11). This was prepared similarly from **7** (91 mg, 0.0480 mmol) in thf (10 mL) and [Ag-

---

[21] Puddephatt, R. J.; Manojlovic-Muir, Lj.; Muir, K. W. *Polyhedron* **1990**, *9*, 2767.

[22] Schoettel, G.; Vittal, J. J.; Puddephatt, R. J. *J. Am. Chem. Soc.* **1990**, *112*, 6400.

[23] Douglas, G.; Jennings, M. C.; Manojlovic-Muir, Lj.; Muir, K. W.; Puddephatt, R. J. *J. Chem. Soc., Chem. Commun.* **1989**, 159.

$(PPh_3)(thf)][PF_6]$ (19 mg, 0.484 mmol; prepared by stirring a solution of $AgPF_6$ and PPh_3 in thf for 10 min) in thf (15 mL) at −78 °C for 0.5 h. Yield: 70%. The complex decomposed rapidly at room temperature.

$[Pt_3(\mu_3\text{-}AuPPh_3)(\mu\text{-}dppm)_3][PF_6]$ (9). To a solution of 7 (121 mg, 0.0642 mmol) in CH_2Cl_2 (10 mL) was added a solution of $[PPh_3Au(thf)][PF_6]$ (67 mg, 0.0645 mmol) in thf (15 mL). After the mixture was stirred for 1 h, it was washed with dilute NaOH (0.05 M, 10 mL), followed by water (25 mL), and dried over $MgSO_4$. Upon filtration and removal of the solvent under reduced pressure, a reddish brown solid was obtained, which was washed with ether (15 mL) and dried under vacuum. Yield: 73%. Anal. Calcd for $C_{93}H_{81}AuF_6P_8Pt_3$: C, 47.7; H, 3.5. Found: C, 46.9; H, 3.6. Mp: 250 °C. MS: calcd for $[Pt_3(\mu_3\text{-}AuPPh_3)(\mu\text{-}dppm)_3]^+$, *m/e* 2197; found, *m/e* 2197.

The same product was formed by reaction of 8 with Et_3N in CH_2Cl_2 solution. The product was isolated and identified by ^{31}P NMR comparison with the above.

Complex 9 was also prepared by reaction of $[Pt_3(\mu_3\text{-}CO)(\mu\text{-}dppm)_3][PF_6]_2$ (80 mg, 0.039 mmol) and $[AuCl(PPh_3)]$ (40 mg, 0.081 mmol) with $NaBH_4$ (2 mg, 0.054 mmol) in MeOH (20 mL) for 2 h. The solvent was evaporated, and the product was extracted with CH_2Cl_2 (5 mL) and precipitated by addition of ether (15 mL). Yield: 95%. This is the preferred synthetic method.

$[Pt_3(\mu_3\text{-}AuPPh_3)_2(\mu\text{-}dppm)_3][PF_6]_2$ (10a). To a solution of 7 (102 mg, 0.0543 mmol) in CH_2Cl_2 (15 mL) was added a solution of $[PPh_3Au(thf)][PF_6]$ (67 mg, 0.1102 mmol) in thf (5 mL). The contents were stirred for 1 h. Reducing the volume of solvent and addition of pentane gave a red solid in 78% yield. Anal. Calcd for $C_{111}H_{96}Au_2F_{12}P_{10}Pt_3$: C, 45.2; H, 3.3. Found: C, 45.6; H, 3.4. MS: calcd for $[Pt_3(\mu_3\text{-}AuPPh_3)_2(\mu\text{-}dppm)_3]^+$, *m/e* 2657; found, *m/e* 2657.

This complex was also prepared (90% yield) by reaction of 9 with $[Ph_3PAu(thf)][PF_6]$ in thf solution.

Reaction of 9 with CF_3COOH. Complex 9 (75 mg, 0.032 mmol) was dissolved in CH_2Cl_2 (0.7 mL), and the solution was placed in an NMR tube (5 mm). To this solution was added by syringe CF_3COOH (2.5 μL, 0.0336 mmol), the tube was sealed, and the contents were mixed thoroughly. The ^{31}P NMR spectral data indicated complete conversion of complex 9 to the complex cation $[Pt_3(\mu_3\text{-}H)(\mu_3\text{-}AuPPh_3)(\mu\text{-}dppm)_3]^{2+}$ **(8).**

$[Pt_3(\mu_3\text{-}AuPMe_3)_2(\mu\text{-}dppm)_3][PF_6]_2$ (10b). To a mixture of $[Pt_3(\mu_3\text{-}CO)(\mu\text{-}dppm)_3][PF_6]_2$ (200 mg) and $[AuBr(PMe_3)]$ (34 mg) in MeOH (20 mL) was added $NaBH_4$ (8 mg). After 2 h of stirring, the solvent was removed, and the product was extracted into thf (10 mL) and then precipitated by addition of ether. Yield: 83%. Anal. Calcd for $C_{81}H_{84}Au_2F_{12}P_{10}Pt_3$: C, 37.8; H, 3.3. Found: C, 37.4; H, 3.8. MS: calcd for $Pt_3(AuPMe_3)_2(dppm)_3^+$, *m/e*, 2284; found, *m/e*, 2283. Fragments corresponding to M − $AuPMe_3$ and M − $2AuPMe_3$ were also detected. Single crystals of **10b** were obtained from toluene/CH_2Cl_2.

Reaction of 10a with PPh_3. To a solution of **10a** (75 mg, 0.025 mmol) in acetone (10 mL) was added PPh_3 (14 mg, 0.0534 mmol). The solution was stirred for 2 h, the solvent evaporated, and the product washed with ether. Characterization by ^{31}P NMR spectroscopy indicated the presence of a 1:1 mixture of complex 9 and $[Au(PPh_3)_2][PF_6]$ [$\delta(^{31}P)$ = 40.1].

Reaction of 9 with CO To Yield 12. Complex 9 (50 mg, 0.0201 mmol) was dissolved in CD_2Cl_2 (0.7 mL), and the solution was placed in an NMR tube (5 mm) fitted with a Teflon tap. Excess CO was condensed into the tube, which was cooled to liquid-nitrogen temperature, and the tap was closed. The ^{31}P NMR spectrum was recorded at −60 °C. After the NMR spectra were recorded, the solvent was removed by bubbling CO into the solution to give a red solid which slowly lost CO at room temperature. IR (Nujol): $\nu(C{\equiv}O)$ 1995 cm^{-1}. Complex **12*** (^{13}CO labeled) was prepared similarly, with the exception that ^{13}CO (99.4% abundant) was used. Following the reaction, a series of ^1H, $^{31}P\{^1H\}$, and $^{13}C\{^1H\}$ NMR spectra were recorded at −60 °C.

X-ray Structure Determination. Slow crystallization from a mixture of toluene and dichloromethane yielded large, dark red crystals of **10b**·2(toluene). A crystal with approximate dimensions 0.29 × 0.25 × 0.16 mm^3 was obtained by cleavage and mounted on a glass fiber in air. The crystal density was determined by neutral buoyancy in a mixture of carbon tetrachloride and dibromoethane. Diffraction measurements were made on an Enraf-Nonius CAD4F diffractometer using prefiltered Cu Kα radiation.[24] The unit cell dimensions were determined and refined by using the angular settings for 20 high-angle reflections. Intensity data were recorded at variable scan speeds so chosen as to optimize counting statistics within a maximum time per datum of 60 s. Background estimates were made by extending the scan by 25% on each side. Three standard reflections were monitored every 180 min of X-ray exposure time and showed only 1.3% decay over the total period of 310.9 h. In all, 13 170 observations and 324 standards were recorded. Corrections were applied for Lorentz, crystal polarization, and background radiation effects, but not for decay, by using the Structure Determination Package[25] running on a PDP11/23+ computer. A numerical absorption correction was applied.[26] Symmetry-equivalent data averaged with *R* = 0.022.

The space group was established from the systematic absences, *h0l* for *l* odd and *0k0* for *k* odd, indicating the monoclinic space group $P2_1/c$ (C_{2h}^5, No. 14). The structure was solved by a combination of the following programs: direct methods using SHELXS-86 running on a SUN 3/50 workstation;[27] least-squares refinement and difference Fourier techniques. Refinement was done by full-matrix least-squares techniques on *F* using the SHELX-76 software.[28] Scattering factors for Au and Pt were taken from ref 29. All the Au, Pt, and P atoms were assigned anisotropic thermal parameters. The hexafluorophosphate anions were constrained to a regular octahedral geometry with *d*(P–F) of 1.60 Å. The

Table IV. Crystallographic Data for $[\mathbf{10b}][PF_6]_2\cdot 2(toluene)$

chem formula $C_{95}H_{100}Pt_3Au_2P_{10}F_{12}$
fw 2758.78
space group $P2_1/c$ (No. 14)
a = 14.442 (2) Å
b = 26.676 (2) Å
c = 25.749 (2) Å
β = 104.117 (8)°
V = 9621 (3) $Å^3$
Z = 4
T = 25 °C
λ = 1.541 84 Å
ρ_{obsd} = 1.95 (5) $g\cdot cm^{-3}$
ρ_{calcd} = 1.904 $g\cdot cm^{-3}$
μ = 157.11 cm^{-1}
transm coeff = 0.323–0.048
$R(F_o)$ = 0.049
$R_w(F_o)$ = 0.088

Table V. Positional (×10^4) and Thermal (×10^3) Parameters for Selected Atoms in **10b**

atom	x	y	z	U,[a] $Å^2$
Au(1)	4572.7 (5)	1234.9 (3)	3740.8 (3)	45.3 (2)*
Au(2)	2645.3 (5)	1351.3 (3)	2051.9 (3)	44.4 (2)*
Pt(1)	3959.0 (4)	795.9 (2)	2744.9 (2)	29.6 (2)*
Pt(2)	4025.5 (4)	1783.9 (2)	2804.0 (2)	30.3 (2)*
Pt(3)	2731.5 (4)	1284.2 (2)	3164.7 (2)	29.6 (2)*
P(1)	5642 (4)	1240 (2)	4524 (2)	53 (1)*
P(2)	1652 (4)	1402 (2)	1233 (2)	57 (2)*
P(3)	5120 (3)	706 (1)	2283 (2)	40 (1)*
P(4)	5319 (3)	1843 (1)	2444 (2)	39 (1)*
P(5)	3705 (3)	2549 (1)	3118 (2)	34 (1)*
P(6)	2188 (3)	1975 (2)	3525 (2)	37 (1)*
P(7)	2069 (3)	562 (1)	3404 (2)	37 (1)*
P(8)	3648 (3)	26 (1)	3036 (2)	35 (1)*
C(10)	5359 (12)	1310 (5)	2017 (7)	47 (4)
C(20)	3136 (10)	2465 (5)	3684 (6)	36 (4)
C(30)	3011 (10)	74 (6)	3590 (6)	37 (4)
C(11)	5868 (17)	1849 (8)	4834 (9)	87 (7)
C(12)	6770 (14)	979 (8)	4512 (8)	79 (6)
C(13)	5327 (18)	893 (9)	5027 (9)	97 (8)
C(21)	492 (15)	1675 (8)	1226 (9)	88 (7)
C(22)	1427 (16)	833 (8)	891 (9)	88 (7)
C(23)	2099 (17)	1766 (8)	759 (9)	89 (7)
C(311)	4803 (8)	298 (4)	1705 (4)	38 (4)
C(321)	6317 (8)	508 (4)	2621 (4)	43 (4)
C(411)	6482 (9)	1858 (5)	2902 (4)	42 (4)
C(421)	5344 (7)	2362 (5)	1989 (5)	52 (4)
C(511)	2904 (8)	2968 (4)	2666 (4)	38 (4)
C(521)	4708 (7)	2958 (4)	3408 (3)	39 (4)
C(611)	1956 (7)	1904 (4)	4182 (5)	40 (4)
C(621)	1151 (8)	2289 (4)	3117 (4)	37 (4)
C(711)	1500 (7)	539 (4)	3963 (5)	36 (4)
C(721)	1157 (9)	267 (4)	2896 (4)	48 (4)
C(811)	4712 (7)	−355 (4)	3333 (3)	44 (4)
C(821)	2891 (8)	−407 (4)	2554 (3)	35 (4)

[a] Parameters marked with an asterisk were assigned anisotropic thermal parameters given as the isotropic equivalent displacement parameter defined as $U_{eq} = {}^1/_3\sum_i\sum_j U_{ij}a_i^*a_j^*a_ia_j$.

---

(24) *Enraf-Nonius CAD4F Users Manual*; Enraf-Nonius: Delft, The Netherlands, 1982.

(25) Enraf-Nonius Structure Determination Package, SDP-PLUS, Version 3.0, 1985.

(26) Coppens, P.; Leiserowitz, L.; Rabinovich, D. *Acta Crystallogr.* **1965**, *18*, 1035.

(27) Sheldrick, G. M. SHELXS-86: Structure Solving Program. University of Gottingen, Germany, 1986.

(28) Sheldrick, G. M. SHELX-76: Program for Crystal Structure Determination. University of Cambridge, England, 1976.

(29) Cromer, D. T.; Liberman, D. *J. Chem. Phys.* **1970**, *53*, 1891.

phenyl rings were constrained to a regular hexagon with d(C–C) of 1.392 Å. All the hydrogen atoms were included in idealized positions [with d(C–H) of 0.95 Å] in structure factor calculations. Common thermal parameters were assigned for methylene and methyl and for phenyl ring hydrogen atoms, and these values were refined.

An inspection of F_o and F_c suggested that an extinction parameter should be included. In the final cycles, employing 8884 observations with $I > 3\sigma(I)$, and weights of the form $w = k/[(\mathrm{sig}\ F_o)^2 + gF_o^2]$, where $k = 0.3564$ and $g = 0.005924$, refinement of 363 variables converged at agreement factors $R = \sum||F_o| - |F_c||/\sum|F_o| = 0.049$ and $R_w = [\sum w(|F_o| - |F_c|)^2/\sum wF_o^2]^{1/2} = 0.088$. The maximum shift/esd of 0.97 was for y of atom C(37). In a total difference Fourier synthesis, there were ten peaks with electron densities in the range 1.911–1.163 e Å^{-3}, and of these, eight were associated with the Au and Pt atoms at distances from 1.03 to 1.19 Å. The extinction parameter refined to 1.41 (14) × 10^{-4}.

The crystal data and experimental conditions are summarized in Table IV and Table SI (supplementary material). Positional and U(equiv) thermal parameters are given for selected atoms in Table V and for all atoms in Table SII (supplementary material). Tables of hydrogen atom parameters, anisotropic thermal parameters, root-mean-square amplitudes of vibration, additional dimensions, a weighted least-squares plane, and structure amplitudes have been deposited as supplementary material (Tables SIII–SVIII).

Acknowledgment. We thank the NSERC of Canada for financial support.

Supplementary Material Available: Tables of X-ray structure determination parameters, positional and thermal parameters, anisotropic thermal parameters, hydrogen atom parameters, root-mean-square amplitudes of vibration, additional interatomic dimensions, and a weighted least-squares plane and dihedral angles (Tables SI–SVII) and figures showing the ^{31}P NMR spectrum (121.4 MHz) of complex **10a**, the ^{31}P NMR spectrum (121.4 MHz) of complex **11**, and the ^{13}C NMR spectrum (75.4 MHz) of complex **12*** (^{13}CO enriched) (Figures S1–S3) (16 pages); a listing of structure amplitudes (Table SVIII) (44 pages). Ordering information is given on any current masthead page.

Contribution from the Department of Chemistry, The University of Tennessee at Chattanooga, Chattanooga, Tennessee 37403,
Department of Chemistry, The University of Alabama in Huntsville, Huntsville, Alabama 35899,
and School of Chemistry, Georgia Institute of Technology, Atlanta, Georgia 30332

Synthesis and Crystal Structure of Bis(1,4,7-trithiacyclodecane)palladium(II) Hexafluorophosphate[1]

Gregory J. Grant,*,† Keith A. Sanders,†,[2] William N. Setzer,‡ and Donald G. VanDerveer§

Received February 21, 1991

We wish to report the synthesis and X-ray crystal structure of the crown thioether complex bis(1,4,7-trithiacyclodecane)palladium(II) hexafluorophosphate, $[\mathrm{Pd(10S3)_2}](\mathrm{PF_6})_2$. The two 10S3 ligands are arranged around the palladium in pseudooctahedral fashion to yield the *meso* stereoisomer. Four of the six sulfur atoms from the 10S3 ligands form a square-planar arrangement around the palladium (mean Pd–S$_{\mathrm{equatorial}}$ bond distance = 2.27 Å). The remaining two sulfurs are coordinated axially at a much greater distance from the Pd (Pd–S$_{\mathrm{axial}}$ = 3.11 Å). Despite this long distance, the axial sulfur atoms do influence the electronic absorption spectrum for the complex resulting in a blue-green solid with a single d–d absorption band at 602 nm. The palladium complex crystallizes with two nitromethane solvent molecules per palladium atom. Crystal data for $[\mathrm{Pd(10S3)_2}](\mathrm{PF_6})_2\cdot 2\mathrm{CH_3NO_2}$: $\mathrm{C_{16}H_{34}PdS_6P_2F_{12}N_2O_4}$, monoclinic, space group $C2/c$; a = 22.473 (9) Å, b = 12.071 (4) Å, c = 11.186 (3) Å, β = 94.14 (3)°, V = 3026.53 Å^3, Z = 4, R = 0.046, D = 1.991 g/cm^3, 2836 reflections measured. The complex undergoes a chemically reversible one-electron oxidation in nitromethane at +1.03 V vs Ag/AgCl.

Introduction

Research involving the coordination chemistry of thioether ligands, especially crown thioethers, is currently very active with several research groups examining the complexation behavior of thioether ligands such as 1,4,7-trithiacyclononane (9S3) and 1,4,7,10,13,16-hexathiacyclooctadecane (18S6) (see Chart I).[3–6] Our research interests have focused on the effects that structural alterations on mesocyclic trithioether ligands might have on the ease of complex formation, complex stability, and complex structure. We have recently reported the synthesis of the 10-membered mesocyclic (medium-sized ring) thioether 1,4,7-trithiacyclodecane (10S3) and presented some complexation studies with divalent first-row transition metals, heavy-metal ions, and zerovalent metals.[7,8] This ligand typically complexes in tridentate fashion forming bis octahedral complexes in which all six sulfur atoms are coordinated. One distinctive feature in the complexation characteristics of 10S3 when compared to 9S3 is that, in the free ligand, one of the sulfur atoms in 10S3 is exodentate while all three sulfur atoms in 9S3 are endodentate.[9] Therefore, the 10S3 ligand has to undergo a conformational change in order to complex as a tridentate ligand whereas the 9S3 ligand does not.

Due to its electronic requirements, palladium(II) typically forms square-planar complexes that are usually yellow-orange in color.[10] Interestingly, Schroder and Wieghardt have independently reported X-ray crystal structures of the $\mathrm{(9S3)_2}$ complex of Pd(II) in which the 9S3 complexes in an unusual pseudooctahedral or $[\mathrm{S_4 + S_2}]$ fashion.[11,12] In the reported structures, four sulfur atoms from two 9S3 ligands form a square-planar arrangement around the Pd (mean Pd–S$_{\mathrm{equatorial}}$ bond length = 2.32 Å) while the two axial sulfur atoms are coordinated at a distance of 2.95 Å from

---

† The University of Tennessee at Chattanooga.
‡ The University of Alabama in Huntsville.
§ Georgia Institute of Technology.

[1] Synthesis and Complexation Studies of Mesocyclic and Macrocyclic Polythioethers. 9. For part 7, see: Grant, G. J.; Grant, C. D.; Setzer, W. N. *Inorg. Chem.* **1991**, *30*, 353. For part 8, see: Setzer, W. N.; Tang, Y.; Grant, G. J.; VanDerveer, D. V. *Inorg. Chem.*, in press. This work was presented in part at the joint 42nd Southeastern Regional Meeting/46th Southwestern Regional Meeting of the American Chemical Society, New Orleans, LA, Dec 5–7, 1990, paper no. 610, and at the 201st National Meeting of the American Chemical Society, Atlanta, GA, April 14–19, 1991; INOR 138.

[2] Undergraduate Research Scholar at The University of Tennessee at Chattanooga, supported by the donors of Petroleum Research Fund, administered by the American Chemical Society.

[3] Schroder, M. *Pure Appl. Chem.* **1988**, *60*, 517.

[4] Blake, A. J.; Schroder, M. In *Advances in Inorganic Chemistry*; Sykes, A. G., Ed.; Academic Press, Inc.: New York, 1990; Vol. 3S, p 2.

[5] Cooper, S. R.; Rawle, S. C. *Struct. Bonding* **1990**, *72*, 1.

[6] Cooper, S. R. *Acc. Chem. Res.* **1988**, *21*, 141.

[7] Grant, G. J.; Carpenter, J. P.; Setzer, W. N.; VanDerveer, D. V. *Inorg. Chem.* **1989**, *28*, 4128.

[8] Setzer, W. N.; Cacioppo, E. L.; Guo, Q.; Grant, G. J.; Kim, D. D.; Hubbard, J. L.; VanDerveer, D. G. *Inorg. Chem.* **1990**, *29*, 2672.

[9] Setzer, W. N.; Guo, Q.; Meehan, E. J., Jr.; Grant, G. J. *Heteroat. Chem.* **1990**, *1*, 425.

[10] Cotton, F. A.; Wilkinson, G. *Advanced Inorganic Chemistry*, 5th ed.; John Wiley and Sons, Inc.: New York, 1988; p 918.

[11] Wieghardt, K.; Kuppers, H.-J.; Raabe, E.; Kruger, C. *Angew. Chem., Int. Ed. Engl.* **1986**, *25*, 1101.

[12] Blake, A. J.; Holder, A. J.; Hyde, T. I.; Roberts, Y. V.; Lavery, A. J.; Schroder, M. *J. Organomet. Chem.* **1987**, *323*, 261.